Supplementary Information

Performance Metrics of Triboelectric Nanogenerator toward Record-High Output Energy Density

Ru Guo[1], Hang Luo[4], Shaoshuai He[2], Xin Xia[2], Tingting Hou[1], Haoyu Wang[1], Chaojie Chen[1], Dou Zhang[4], Yunlong Zi*[1,2,3]

1 Department of Mechanical and Automation Engineering, The Chinese University of Hong Kong, Shatin, N.T. Hong Kong, China

2 Thrust of Sustainable Energy and Environment, The Hong Kong University of Science and Technology (Guangzhou), Nansha, Guangzhou, Guangdong, 511400, China

3 Guangzhou HKUST Fok Ying Tung Research Institute, Nansha, Guangzhou, Guangdong 511457, China

4 Powder Metallurgy Research Institute, State Key Laboratory of Powder Metallurgy, Central South University, Changsha, 410083, Hunan Province, China

Correspondence: ylzi@hkust-gz.edu.cn

Supplementary Note 1. Theoretical maximum output energy density limited by dielectric breakdown in SFT-TENG.

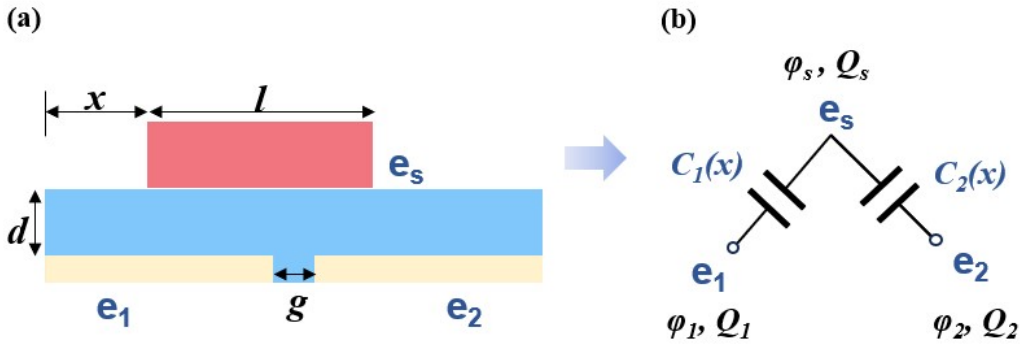

Supplementary Figure 1. (a) Physical structure and (b) electric model of SFT-TENG with critical parameters.

As shown in Supplementary Figure 1, a simplified physical and electric model of SFT-TENG was constructed to explore the maximized output energy density limited by dielectric breakdown in SFT-TENG.

When the slider moves onto the left electrode, i.e., the movement distance (x) x=0, at the open-circuit state, the electrical potential difference between the two output electrodes is zero, given as follow:

$$V_{21} = \varphi_2 - \varphi_1 = 0 \qquad (1)$$

Here, the capacitance (C_1) between slider dielectric and left output electrode is described as follow:

$$C_1(x = 0) = \frac{\varepsilon_0 \varepsilon_r l w}{d} \qquad (2)$$

Where ε_0 and ε_{ri} are vacuum permittivity and relative permittivity of dielectric layer,

and l, w, and d are electrode length, width, and stator dielectric thickness, respectively. Meanwhile, the capacitance ($C_2(x=0)$) between slider dielectric and right output electrode will be very small, about 10^{-3}~10^{-4} $C_1(x=0)$.

The charge amount on the slider surface (Q_s) is given by multiplying the charge density (σ) by the area according to the equation:

$$Q_s = \sigma l w \tag{3}$$

Hence, the charge amount between capacitance C_1 and C_2 can be described as following formula, where β is the proportionality coefficient:

$$Q_1 = \frac{-Q_s C_1(x=0)}{C_1(x=0) + C_2(x=0)} \approx \sigma l w \beta, \quad (\beta \sim 99.9\%) \tag{4}$$

$$Q_2 = -Q_s + Q_1 = -\sigma l w (1-\beta) \tag{5}$$

When slider moves displacement of x_0, i.e., at $x=x_0$ ($x_0>g$), Q_1 and Q_2 keep open-circuit state, the $C_1(x=x_0)$ and $C_2(x=x_0)$ will be expressed as:

$$C_1(x=x_0) = \frac{\varepsilon_0 \varepsilon_r (l-x_0) w}{d} \tag{6}$$

$$C_2(x=x_0) = \frac{\varepsilon_0 \varepsilon_r (x_0-g) w}{d} \tag{7}$$

Hence, according to the equation (4-7), the corresponding voltage on $C_1(x=x_0)$ and $C_2(x=x_0)$ is present, respectively:

$$V_{s1} = \frac{-Q_1}{C_1(x=x_0)} = \frac{\sigma l d \beta}{\varepsilon_0 \varepsilon_r (l-x_0)} \tag{8}$$

$$V_{s2} = \frac{-Q_2}{C_2(x=x_0)} = \frac{\sigma l (1-\beta) d}{\varepsilon_0 \varepsilon_r (x_0-g)} \tag{9}$$

So, the electric potential difference between two output electrodes is expressed as:

$$V_{12} = V_{oc}(x = x_0) = V_{s1} - V_{s2} = \frac{\sigma l d}{\varepsilon_0 \varepsilon_r}\left(\frac{\beta}{l - x_0} - \frac{1-\beta}{x_0 - g}\right) \quad (10)$$

We assume the energy output of SFT-TENG is mainly limited by dielectric breakdown. The following unequal relationship should be meet:

$$V_{s1} \le E_b d \quad (11)$$

Where E_b is electric breakdown strength of the stator dielectric.

From equation (8, 11), the charge density can be expressed as:

$$\sigma \le \frac{\varepsilon_0 \varepsilon_r E_b (l - x_0)}{l\beta} \approx \frac{\varepsilon_0 \varepsilon_r E_b (l - x_0)}{l} \le \frac{\varepsilon_0 \varepsilon_r E_b (l - g)}{l} \quad (12)$$

From equations (9,10),

$$V_{12} \le E_b (l - x_0) d\left(\frac{\beta}{l - x_0} - \frac{1-\beta}{x_0 - g}\right) \approx E_b d\beta \quad (13)$$

Hence, the energy density of half-cycle ($U_{half\text{-}cycle}$) defined as the energy output (E) per unit volume (V) can be described as:

$$U_{half-cycle} = \frac{E}{V} = \frac{Q_s V_{12}}{(2l + g)wd} \quad (14)$$

Combining equations (3, 13), the $U_{half\text{-}cycle}$ is given as follow:

$$U_{half-cycle} = \frac{V_{12}\sigma l}{w(2l + g)d} \le \varepsilon_0 \varepsilon_r E_b^2 \left(\frac{l - g}{2l + g}\right) \quad (15)$$

Considering the inevitable energy loss caused by dielectric loss, a parameter of loss factor ($tan\delta$) is introduced here. Therefore, the equation (15) is revised as follow:

$$U_{half-cycle} \le (1 - tan\delta)\varepsilon_0 \varepsilon_r E_b^2 \left(\frac{l - g}{2l + g}\right) \quad (16)$$

In addition, regarding to structural parameters of SFT-TENG, the gap distance (*g)* between two output electrodes cannot be too small, otherwise it may cause gap discharge. In order to avoid gap breakdown, the following relationship is needed:

$$\frac{V_{12}}{g} \leq E_b \qquad (17)$$

From equation (11), it can be seen:

$$V_{12} \approx \frac{\sigma d l}{\varepsilon_0 \varepsilon_r (l - x_0)} \qquad (18)$$

Hence, gap distance *g* needs to be met:

$$g \geq d \frac{\sigma \quad l \quad 1}{\varepsilon_0 \varepsilon_r l - x_0 E_d} \qquad (19)$$

In mathematical analysis,

$$g > d \frac{\sigma \quad l \quad 1}{\varepsilon_0 \varepsilon_r l - g E_d} \qquad (20)$$

Let $A_0 = \frac{d \quad \sigma \quad 1}{l \, \varepsilon_0 \varepsilon_r E_d}$, the equation (20) is expressed as:

$$g^2 - lg + A_0 l^2 < 0 \qquad (21)$$

Then, *g* is solved as:

$$\frac{l + \sqrt{l^2 - 4A_0 l^2}}{2} > g > \frac{l - \sqrt{l^2 - 4A_0 l^2}}{2} \qquad (22)$$

Considering $d \ll l$; $\sigma \sim \varepsilon_0 \varepsilon_r E_b$, $A_0 \ll 1$, there is an unequal relationship as follows:

$$l > g > 2A_0 l \approx 2d \qquad (23)$$

So, the equation (16) is expressed as:

$$U_{half-cycle} \leq \frac{1}{2}(1 - tan\delta)\varepsilon_0 \varepsilon_r E_b^2 \left(\frac{l - 2d}{l + d}\right) \qquad (24)$$

Finally, the energy density in one cycle of movement can be obtain as follow:

$$U_{one-cycle} \leq (1 - tan\delta)\varepsilon_0\varepsilon_r E_b^2\left(\frac{l-2d}{l+d}\right) \quad (25)$$

It can be concluded that the maximized output energy density of SFT-TENG is mainly influence by the material characteristics of relative permittivity (ε_r), loss factor ($tan\delta$) and breakdown strength (E_b); and the structural factors of electrode length, dielectric thickness, etc.

Supplementary Note S2. Theoretical charge density of SFT-TENG under high-voltage excitation.

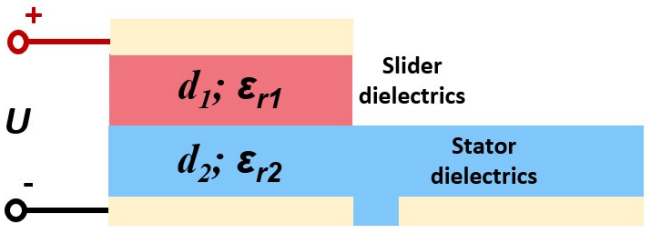

Supplementary Figure 2. The structure model of SFT-TENG under high-voltage excitation.

As shown in Supplementary Figure 2, when the slider moves onto one of the output electrodes, the equivalent circuit of SFT-TENG could be regarded as parallel plate capacitance model. The capacitance (C) of the TENG is described as follow:

$$\frac{1}{C}=\frac{1}{C_1}+\frac{1}{C_2} \tag{26}$$

Where the C_i (i=1, 2) can be given as follow:

$$C_i=\frac{\varepsilon_0\varepsilon_{ri}S}{d_i} \tag{27}$$

Where ε_0 and ε_{ri} are vacuum permittivity and relative permittivity of dielectric layer, respectively, and d_i is thickness of dielectric, S is the area of the electrode area.

So, the capacitance of TENG (C) is described as follow:

$$C=\frac{\varepsilon_0 S}{(\frac{d_1}{\varepsilon_{r1}}+\frac{d_2}{\varepsilon_{r2}})} \tag{28}$$

Then, according to the charge conservation:

$$CU=\sigma S \tag{29}$$

Where U is external applied voltage, σ is the surface charge density.

Hence, the σ can be described as follow:

$$\sigma = \frac{\varepsilon_0 U}{\left(\frac{d_1}{\varepsilon_{r1}} + \frac{d_2}{\varepsilon_{r2}}\right)} \tag{30}$$

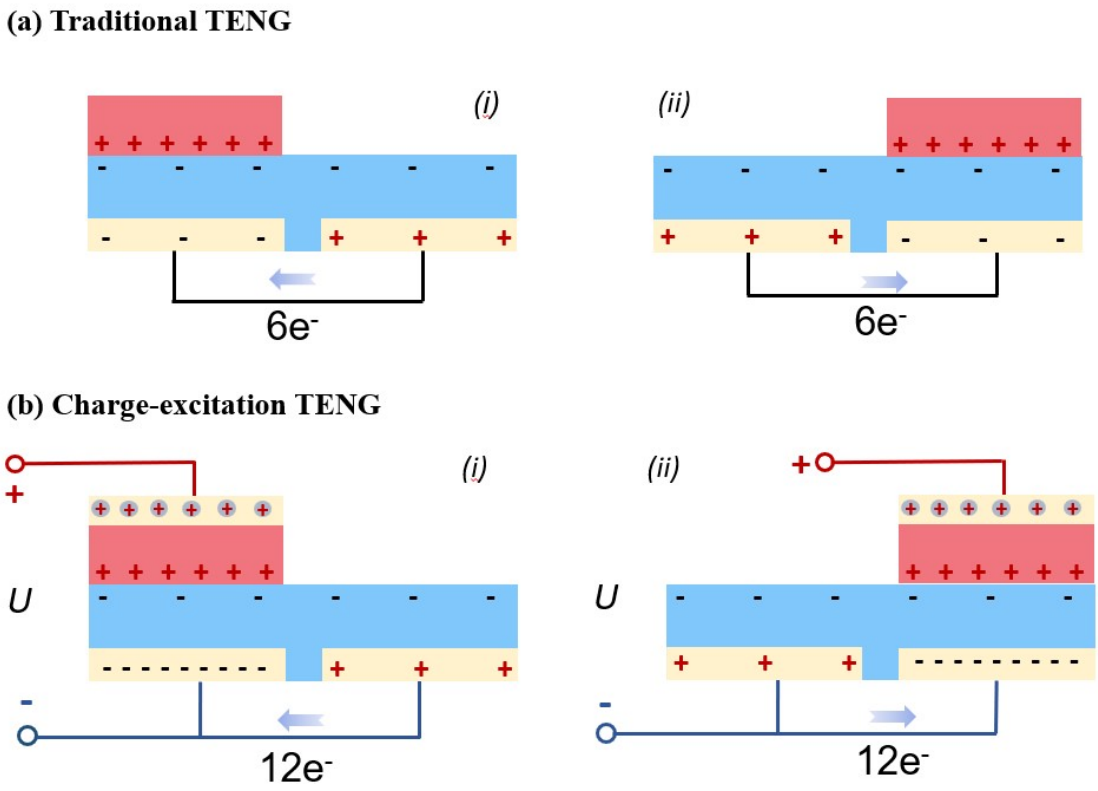

Supplementary Figure 3. Charge transferring mechanism for (a) traditional TENG and (b) charge-excitation TENG.

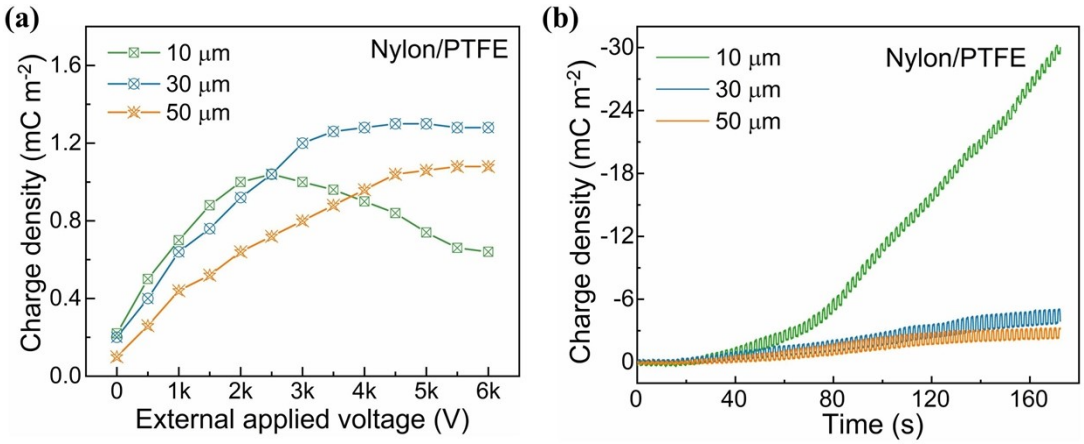

Supplementary Figure 4. (a) Charge excitation curve and (b) charge density of SFT-TENG (Nylon/PTFE pair) with different PTFE film thickness.

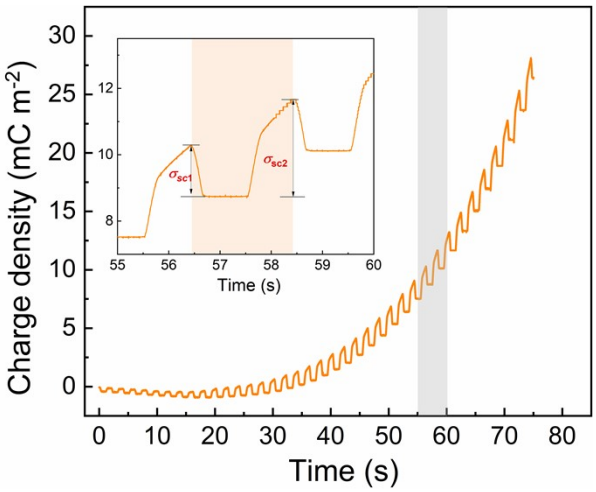

Supplementary Figure 5. Charge density curve of SFT-TENG with leakage effect. Considering the voltage-charge (*V*-*Q*) plot per cycle to quantify the maximized output energy density, the charge density generated during two half-cycles was defined as σ_{sc1} and σ_{sc2}, respectively.

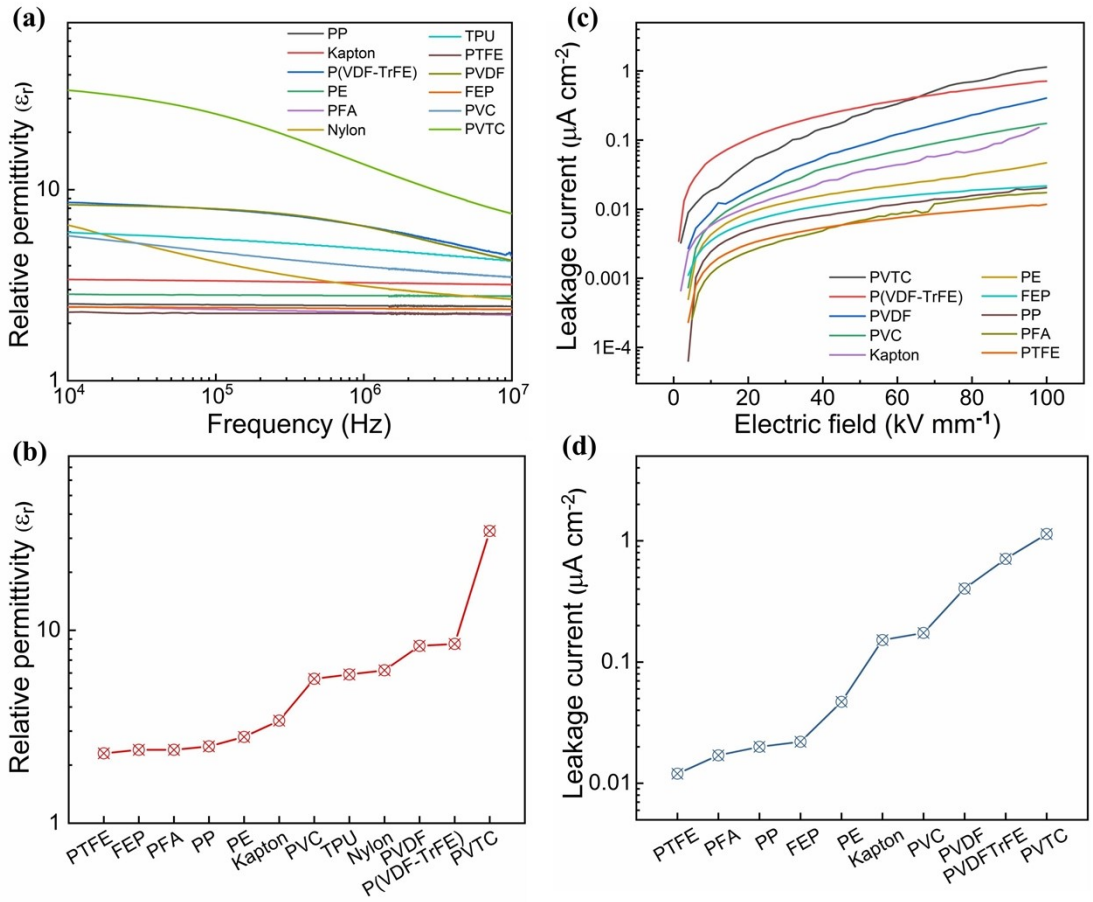

Supplementary Figure 6. (a) Frequency dependence of relative permittivity for different dielectrics used in SFT-TENG. (b) Comparison of relative permittivity at 10 kHz. (c) Leakage current density of different dielectrics under high electric field. (d) Comparison of leakage current density at the same electric field of 100 kV mm^{-1}.

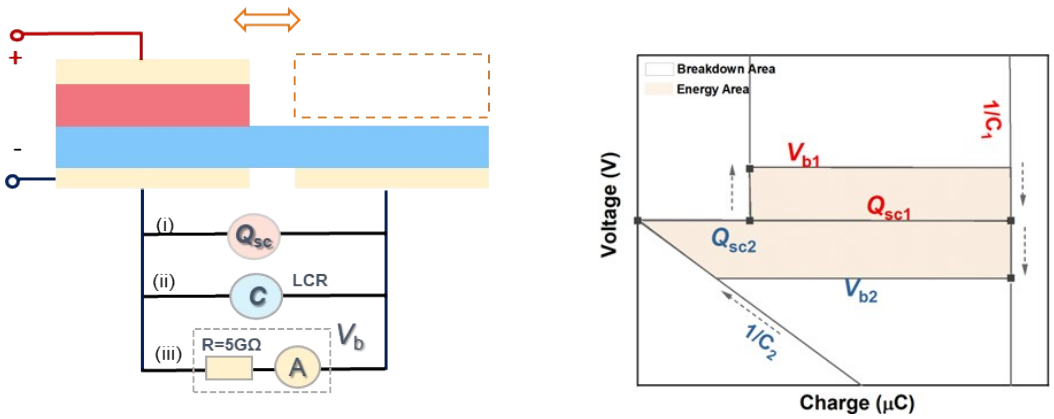

Supplementary Figure 7. (a) Test circuit schematic diagram for the key parameters (Q_{sc}, $V_{b,}$ and C) of the *V*-*Q* plot. (b) The revised *V*-*Q* plot of SFT-TENG under the effect of charge excitation for the determination of the maximized output energy density.

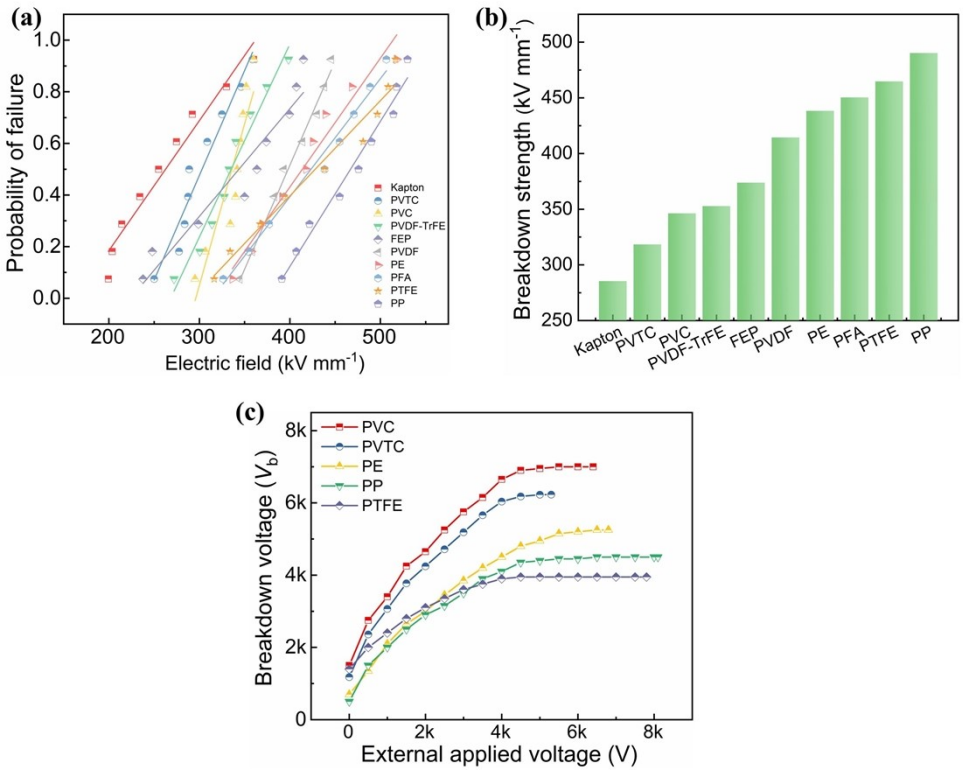

Supplementary Figure 8. (a) Characterization of dielectric breakdown strength by Weibull distribution (b) Comparison of intrinsic breakdown strength (E_b) of dielectrics. (c) Relationship curve of breakdown voltage V_b and external applied voltage of several typical dielectrics.

Characterization of intrinsic breakdown strength of dielectric materials: A two-parameter Weibull cumulative probability function was used to analyze the E_b of 10 kinds of tribomaterials as the following equation:

$$P(E) = 1 - exp[-(E/E_b)^{\beta}] \quad (31)$$

where $P(E)$ is the cumulative failure probability, E is the breakdown strength obtained through experimental tests. The characteristic breakdown strength E_b refers to the field strength when the breakdown probability is 63.2%. The E_b of each dielectric was obtained from a fit using Weibull failure statistics across 9 test samples (Supplementary Figure 8a). Then the comparison of all the E_b values was present in Supplementary

Figure 8b. As a whole, the linear dielectrics with low-permittivity, like PP, PTFE, PFA, etc., possess higher E_b values than those nonlinear dielectrics with high permittivity, like kapton, PVTC, PVC, etc.

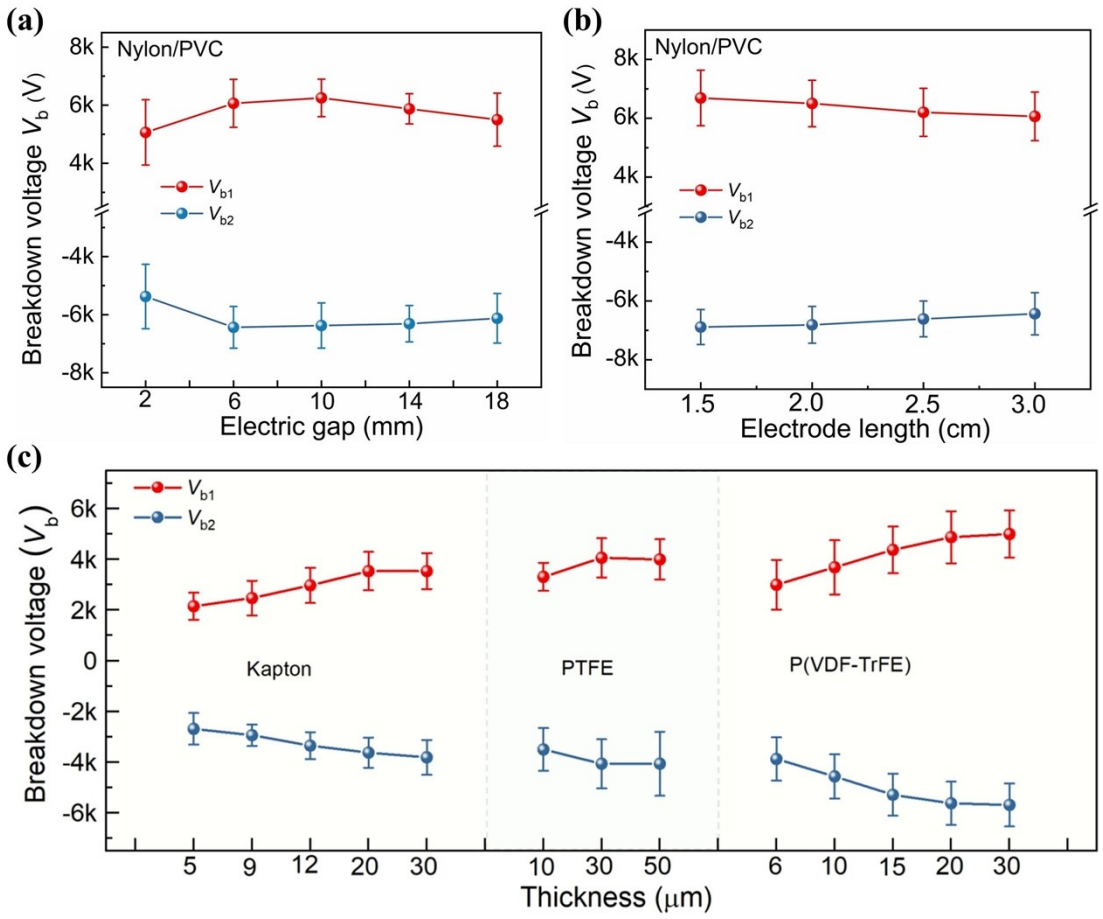

Supplementary Figure 9. Breakdown voltage of SFT-TENG with different structural factors: (a) electrode gap, (b) electrode length, (c) film thickness.

The effect of structure factors on the breakdown voltage: The influence of structure factors on the V_b of TENG was discussed here. In Supplementary Figure 9a, with an enlarging electrode gap from 2 mm to 18 mm, both V_{b1} and V_{b2} show a trend of first increasing and then slightly decreasing with an optimal distance obtained at 6 mm. Too

small or large gap distance is not desirable because of increasing the possibility of gap breakdown discharge and decreasing charge density, respectively. Besides, Supplementary Figure 9a shows increasing electrode length easily reduces the V_{b1} and V_{b2}, which is attributed to the fact that the larger electrode area covers more internal defects in the dielectric, making it easier to induce dielectric breakdown. Finally, an obvious decline of V_{b1} and V_{b2} was observed in Supplementary Figure 9c for all three dielectric of Kapton, PTFE, and P(VDF-TrFE) with the reduction of film thickness, which could explained by the enhanced exerted electric field and increased leakage conductivity from thinner dielectric.

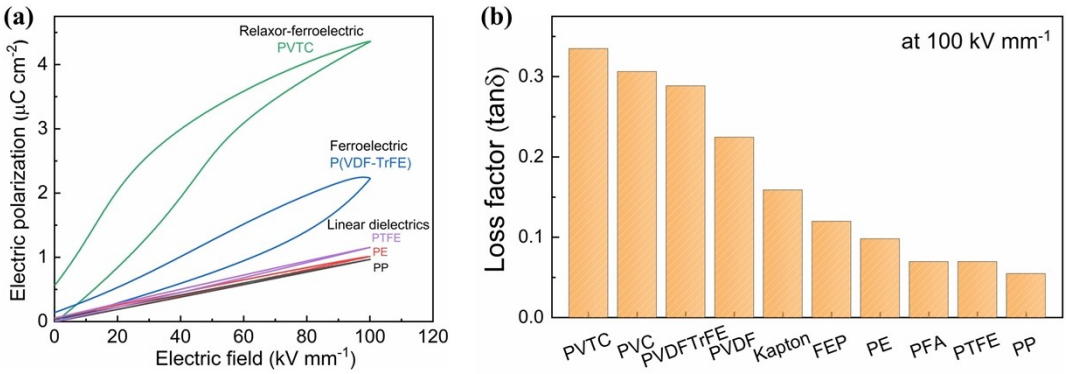

Supplementary Figure 10. (a) Polarization hysteresis loops of representative triboelectric polymers. (b) Loss factor (tanδ) of different dielectrics.

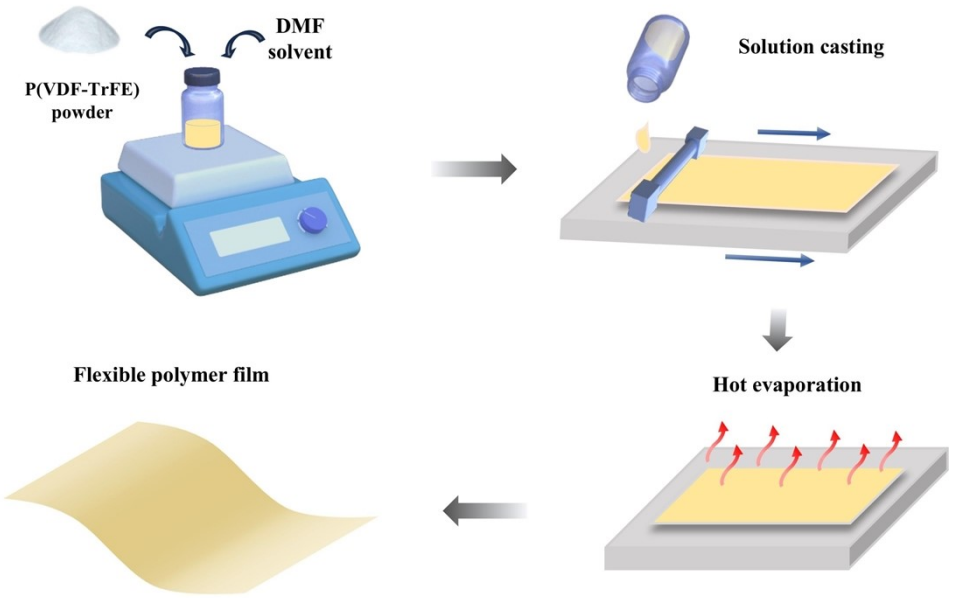

Supplementary Figure 11. Scheme of the preparation of stretched P(VDF-TrFE) film.

Preparation of stretched P(VDF-TrFE) film: Firstly, the raw P(VDF-TrFE) powders were proportionally (10 wt.%) added in N, N-dimethylformamide solvent and stirred at 60℃ for 6h until fully dissolved. Then the solution was poured on a clear glass substrate followed by tape casting by a scraper with a clearance of 400 μm. After drying at 80℃ for 12h to volatilize the solvent, the P(VDF-TrFE) polymer films with a thickness of ~20 μm were obtained. Then, the films were cut into samples of 80×100 mm^2 size, and both ends were clamped on a customized uniaxial drawing machine. The P(VDF-TrFE) films with stretch ratios R (final length to initial length) of three were obtained at a drawing speed of 12 mm s^{-1}) and temperature of 100 ℃ and then served as tribomaterials to fabricate TENG device.

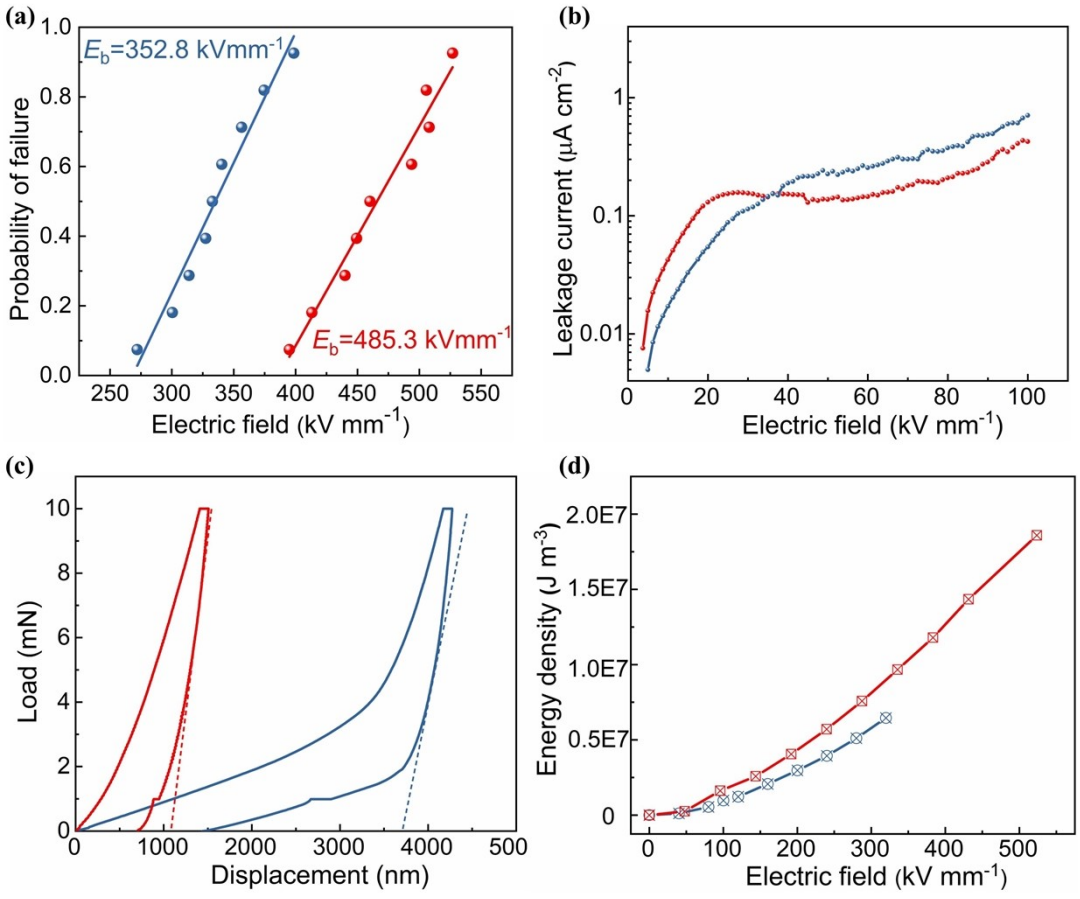

Supplementary Figure 12. Material characterization. (a) Electric breakdown strength, (b) Leakage current density, (c) Young's modulus, (d) Intrinsic energy storage density of the P(VDF-TrFE) film before and after uniaxial stretching.

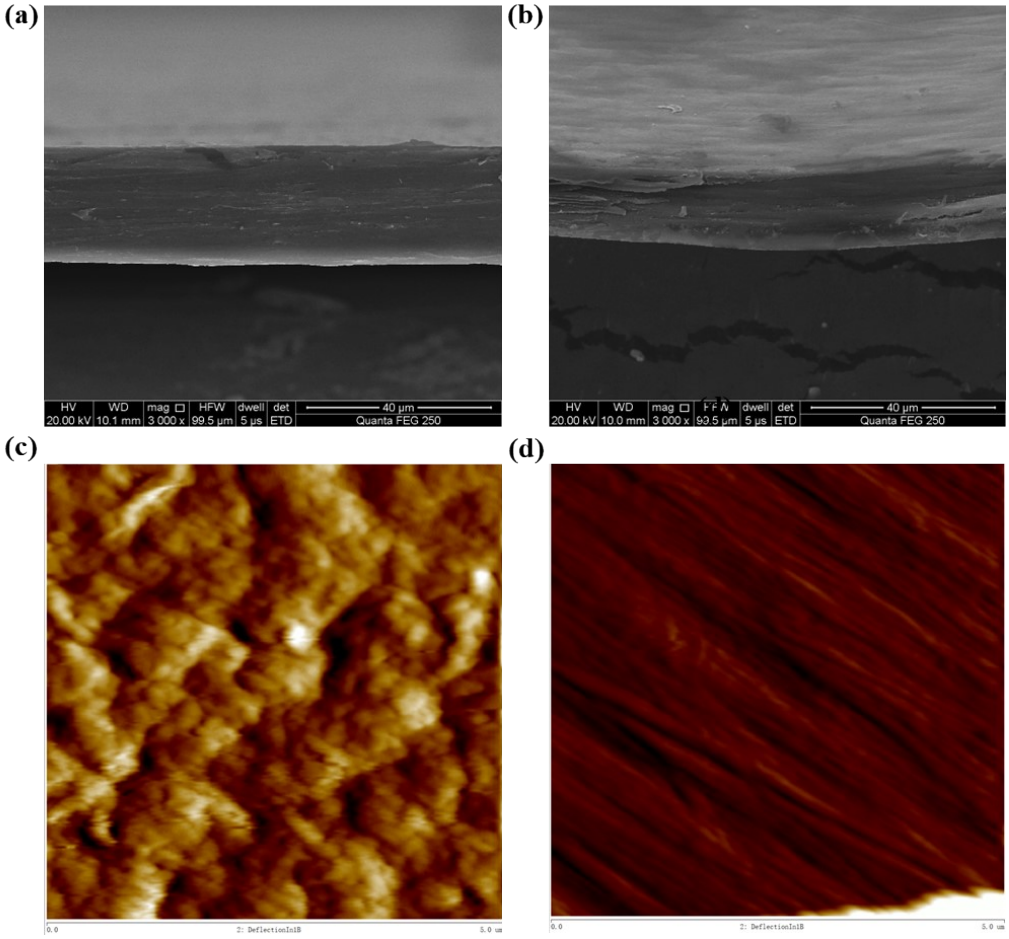

Supplementary Figure 13. (a, b) SEM images of P(VDF-TrFE) film before and after uniaxial stretching to characterize cross-section thickness. (c, d) AFM images of P(VDF-TrFE) film before and after uniaxial stretching to characterize surface morphology.

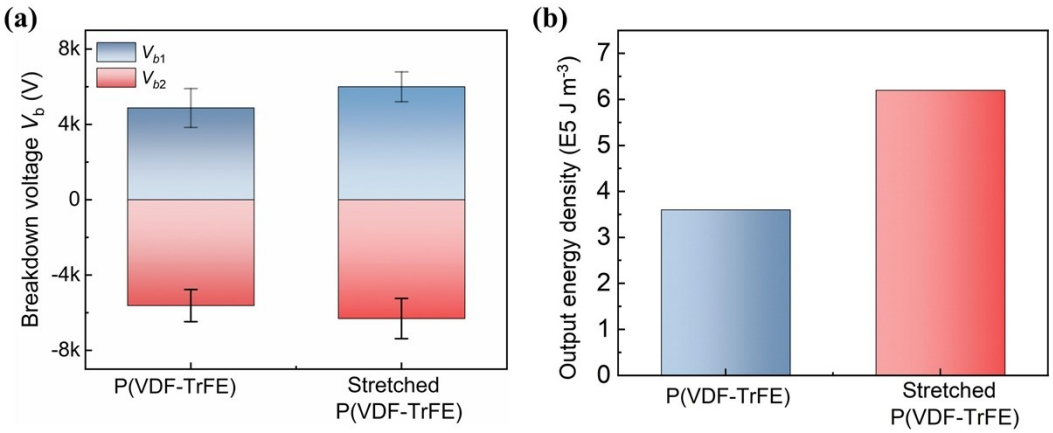

Supplementary Figure 14. Comparison of output performance. (a) Breakdown voltage, (b) Maximized output energy density of the TENG with Nylon/P(VDF-TrFE) film before and after uniaxial stretching.

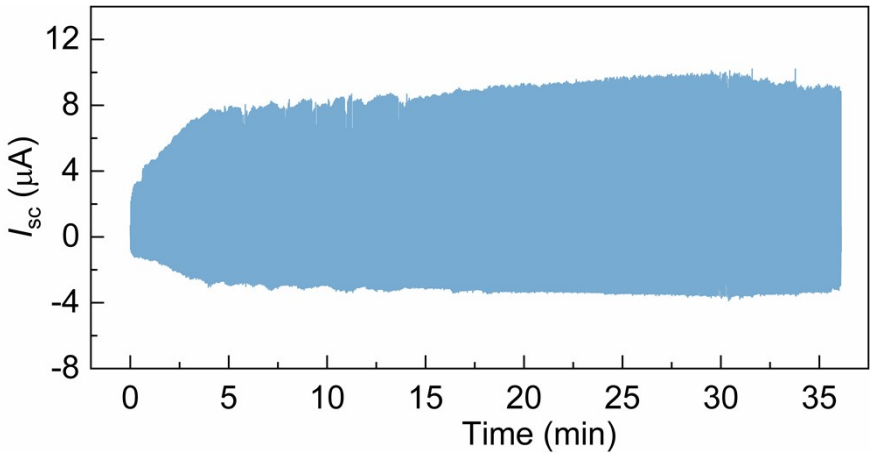

Supplementary Figure 15. The long-term stability of SFT-TENG using stretched P(VDF-TrFE) film as stator dielectric.

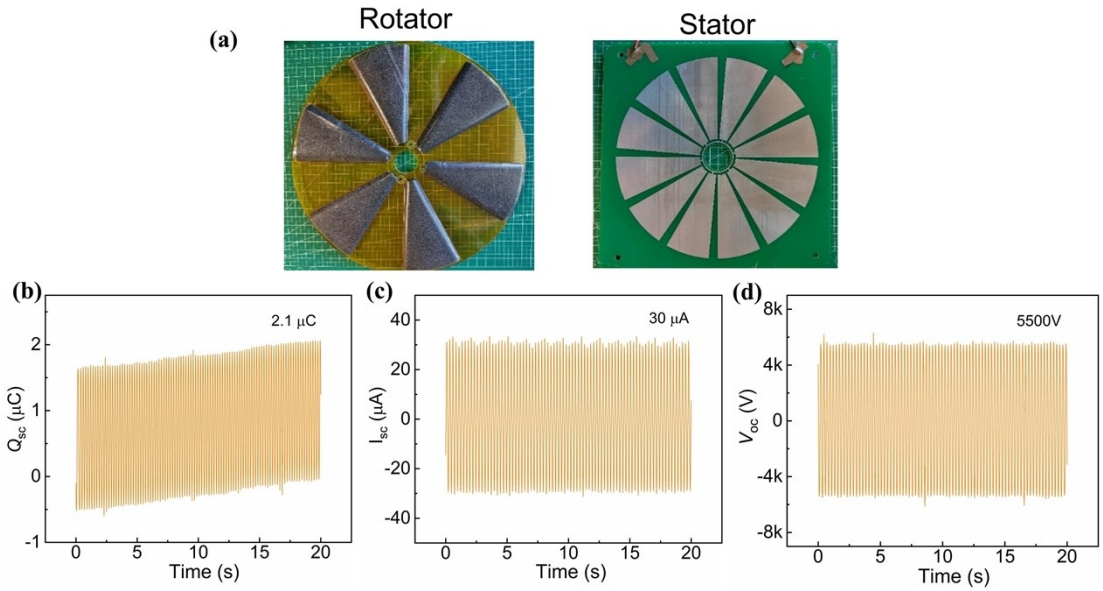

Supplementary Figure 16. (a) Photographs of the rotator and stator components of excitation-TENG. (b) Short-circuit charge Q_{sc}, (c) Short-circuit charge I_{sc}, and (d) Open-circuit voltage V_{oc} of excitation-TENG.

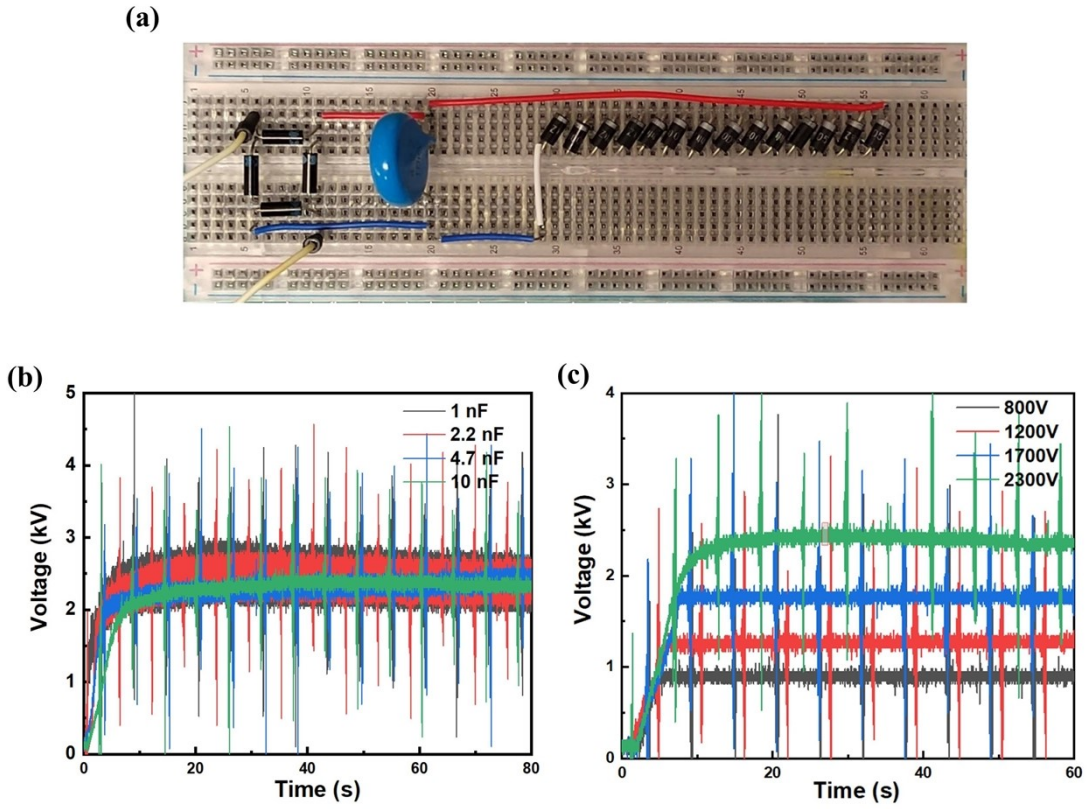

Supplementary Figure S17. (a) Photographs of the external management circuit. Voltage performance of excitation TENG with different (b) buffer capacitors and (c) Zener diodes in circuit.

Supplementary Table 1 Key parameters for the plot of the *V*-*Q* curve to evaluate the maximized output energy density of SFT-TENG with different stator dielectrics.

	Material	Q_{sc1} (μC)	Q_{sc2} (μC)	V_{b1} (V)	V_{b2} (V)	Thickness (μm)
1	PTFE	1.3	-1.4	4125	-4437.5	30
2	FEP	0.9	1.6	3687.5	-4062.5	20
3	PVC	2.1	4.3	6250	-6375	40
4	PVDF	1.2	2.8	4662.5	-5000	22
5	P(VDF-TrFE)	2.0	4.1	4875	-5625	20
6	P(VDF-TrFE-CTFE) (PVTC)	2.2	3.8	5737.5	-6000	20
7	Kapton	0.7	-1.0	3600	-3812.5	25
8	PFA	1.4	1.5	4625	-5500	35
9	PE	1.36	1.5	4625	-4875	25
10	PP	1.1	1.5	4312.5	-4687.5	25
11	Nylon	Slider dielectric				25

Supplementary Table 2. Summary of the key indexes of dielectric materials for the performance evaluation of charge density and output energy density.

Material	σ_i (mC m^{-2})	σ_i*	ε_r	ε_r*	1-Tanδ	(1-Tanδ)*	E_b (kV mm^{-1})	E_b*	σ_{sc} (mC m^{-2})	U_m (10^5 J m^{-3})
PVTC	0.55	0.92	32.7	1	0.66	0.69	318.0	0.65	2.2	4.3
PVC	0.60	1	5.6	0.17	0.75	0.79	346.0	0.71	2.3	3.8
P(VDF-TrFE)	0.46	0.76	8.5	0.26	0.71	0.75	352.8	0.71	2.0	3.6
PVDF	0.32	0.53	8.3	0.25	0.78	0.82	414.4	0.85	1.4	2.1
PE	0.13	0.21	2.7	0.08	0.9	0.95	438.3	0.89	1.2	1.4
PFA	0.34	0.57	2.4	0.07	0.93	0.98	450.2	0.92	1.3	1.2
PP	0.11	0.19	2.5	0.08	0.95	1	490.2	1	1.0	1.2
FEP	0.41	0.69	2.4	0.07	0.88	0.93	373.9	0.76	0.8	1.1
PTFE	0.43	0.72	2.3	0.07	0.93	0.98	464.9	0.95	1.2	0.9
Kapton	0.31	0.52	3.4	0.10	0.84	0.88	285.9	0.58	0.7	0.7
Stretched P(VDF-TrFE)	0.55	0.92	14.9	0.46	0.65	0.68	485.3	0.99	2.8	6.2

*Noted: The material parameters marked with * represent the normalized values.*

Supplementary Table 3. Comparison of multiple parameters and output performance among recently reported TENG.

	Structure Mode	Design Strategy	Dielectric material	Charge density ($mC\ m^{-2}$)	Output voltage (V)	Output energy density ($J\ m^{-3}$)	Refs.
1	SFT (Rotary)	Floating self-excited	25μm nylon; 30μm PTFE	0.071	470	1.2×10^3	Nat. Commun. 2021, 12:4689.
2	SFT (Sliding)	Non-contact mode	50μm PTFE	0.26	3879	1.4×10^4	Adv. Energy Mater. 2022, 12, 2201708.
3	SFT (Sliding)	Liquid suspension	25μm nylon; 25μm nylon	0.704	4200	5.4×10^4	Adv. Mater. 2022, 2209657.
4	SFT (Sliding)	Charge space-accumulation	25μm nylon; 50μm PTFE	1.63	3000	2.6×10^4	Nat. Commun. 2020, 11:4277.
5	SFT (Sliding)	Charge pumping	50μm PET; 50μm Kapton	1.328	1400	3.7×10^4	Adv. Energy Mater. 2021, 11, 2101147.
6	SFT (Sliding)	Charge migration for volume effect	1mm PU; 100μm FEP	0.37	3000	9.9×10^2	Adv. Mater. 2023,2302954.
7	SFT (Sliding)	Charge reversion process	30μm PI	0.78	-	6.1×10^3	Energy Environ. Sci., 2023,16, 5294-5304.
8	CS	Self-Polarization Effect	7.5μm $BaTiO_3$/PVDF	1.67	600	3.6×10^3	Adv. Funct. Mater. 2022, 2204322.
9	CS	Polar High-k Material	0.1wt%PZT/ PVDF	3.53	900	3.6×10^4	Adv. Mater. 2022, 34, 2109918.
10	CS	Charge trapping failure	10μm, CP/PVDF	4.13	700	5.8×10^4	Energy Environ. Sci., 2023,16, 2274-2283.
11	CS	Ultra-fast charge self-injection technique	PVDF-TrFE	2.67	700	2.5×10^5	Adv. Mater. 2024,36,2312148.
12	CS	Suppressing air breakdown and	7μm PVDF+PI	2.2	1385	8.0×10^4	Adv. Energy Mater. 2024,

		dielectric leakage					14,2303874.
13	CS	Annealing treatment	8μm Annealed PVTC	8.6	600	1.01×10^5	Energy Environ. Sci., 2024,17, 3819-3831.
14	CS	Inhibiting charge injection and dielectric loss	PZT5H+PVTC 1mm+5μm	2.83	750	4.2×10^3	Adv. Energy Mater. 2024, 2400429.
15	SFT (Sliding)	Charge excitation	14μm Stretched P(VDF-TrFE)	2.8	6000	6.2×10^5	**This work**